Solar Energy Materials 10 (1984) 209–221
North-Holland, Amsterdam

POLYCRYSTALLINE SILICON RIBBONS FOR SOLAR CELLS PREPARED BY FAST COOLING

C.F.A. van OS, J.L.P.W. VERPALEN and J. BEZEMER

Technical Physics Department, State University Utrecht, P.O. Box 80 000, 3508 TA Utrecht, The Netherlands

Received 24 February 1984

Experiments on the production of 0.1 mm thick polycrystalline silicon ribbons by jet casting and flow casting are reported. The processes are described with models for heat transport and momentum transport. Attention is paid to process stability. Grain growth, which is necessary for solar cell applications, has been studied. The activation energy for grain growth amounted to (4.4 ± 0.7) eV.

1. Introduction

The impingement of a flow of liquid material on a fast spinning wheel, a disk or set of rollers is a commonly used method to produce amorphous metal alloys. Due to the fast cooling the metal alloys freeze into a glassy state.

When silicon is cast in this way, no amorphous but polycrystalline ribbons are produced. The mean grain size is rather small but this size can be improved by grain growth, which occurs during annealing close to the melting temperature. Provided a sufficiently large grain size can be obtained, the casting technique is a very promising method for production of solar cells. When a stable casting process can be achieved, combined with a method for fast ribbon handling, ribbons of various dimensions can be produced with a speed of about 10 m/s.

First experiments on cast silicon were reported by Arai et al. [1] who also made some cells of the as grown ribbons. Another possible application of the casting technique for solar cells was suggested by Raman and Witt [2] who made laminated layers of a semiconducter on top of a glassy metal (e.g. InSb on a-Cu_x Zr_y). In this way the handling problems of the brittle ribbons are reduced by the strength of the metal layer.

In this paper, we distinguish between two processes, which we will call jet casting and flow casting. In both cases, molten silicon is pressed out of a fused quartz tube. In the case of jet casting, the tip of the quartz tube is at a distance of several mm from the cooling wheel. A silicon jet flows from the tube to the wheel, and a semistationary liquid puddle is built up on top of the cooling surface. A solid ribbon develops at the interface. This continuously growing ribbon is carried away by the rotating wheel. Additionally on the top of the ribbon some liquid silicon may be dragged out of the puddle too. The thickness of the liquid silicon layer is determined

by the momentum transport from the wheel to the puddle. This momentum transport can be characterized by the thickness of a flow boundary layer. In the case of flow casting, the tip of the quartz tube is only about 0.2 mm away from the cooling wheel. Liquid silicon fills the space between the tube and the wheel which affects the dimensions of the ribbon.

Due to the crystallization, the fast casting processes of silicon differ considerably from fast casting of amorphous metal alloys. Firstly, the large melting heat governs the solidification in the puddle. Secondly, the formation of crystals influences the homogeneity of the ribbon e.g. by roughening the solid liquid interface. Only for jet casting of amorphous alloys many references are available in literature. Kavesh [3] gives the principles of fabrication, Anthony and Cline [4] pay much attention to the stability of the jet and Hideo Shingu et al. [5] give computations on the momentum transport in the puddle. Pavuna [6] and Liebermann [7] describe how the stability of the process can be enhanced by a forced gas flow around the jet and the puddle.

2. The jet casting process

A schematic representation of jet casting is shown in fig. 1. A liquid silicon jet flows into a puddle on top of the cooling wheel surface. This surface drags the solid ribbon out of the puddle. The jet is forced out of the tube by an applied pressure Δp of 25 to 200 mbar, depending on the length a and the radius R of the orifice of the tube. The Reynolds number has to be selected within the range

$$50a/R < \mathrm{Re} < 2000, \tag{1}$$

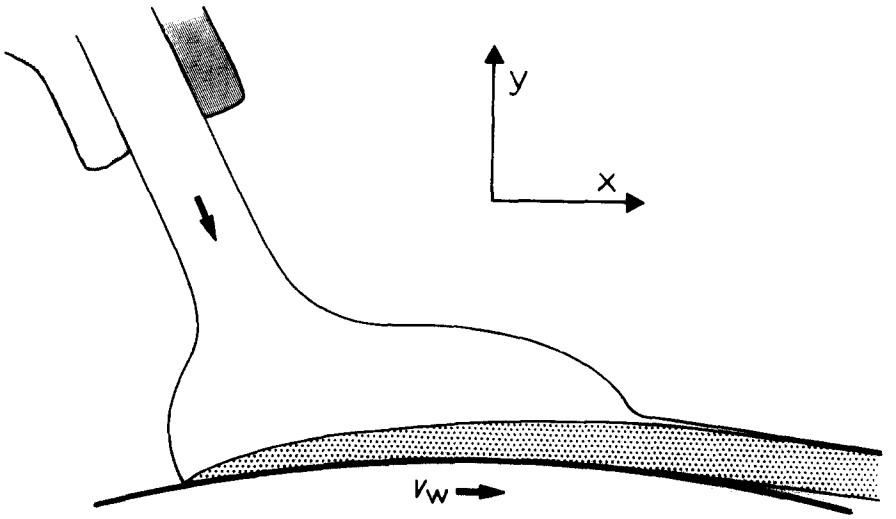

Fig. 1. Schematic representation of jet casting, showing the silicon jet, the puddle and the solid ribbon on top of the spinning wheel.

so that a laminar flow is obtained which obeys Bernoulli's law. The mass flow Q of the liquid silicon is then approximately given by

$$Q = \pi R^2 \rho_1 v_j = \pi R^2 (2\rho_1 \Delta p)^{1/2}. \tag{2}$$

For a stable process, this mass flow has to be equal to the mass of the ribbon produced per unit time. On the other hand, the dimensions of the ribbon are determined by the size of the puddle and by the transport of heat and momentum in the puddle.

To describe the ribbon production in the puddle, we will first discuss the balance of heat. Since the change in enthalpy of silicon during solidification is very large, the growth of the solid layer at the bottom of the puddle is mainly governed by the thermal conduction of the solidification heat through the solid ribbon to the wheel. In the temperature range of interest, the heat conductivity $\lambda(T)$ of solid silicon as a function of the temperature T in kelvin is by a good approximation

$$\lambda(T) = k/T \quad \text{and} \quad k = 350 \text{ W/cm}. \tag{3}$$

Considering only heat transport through the growing ribbon in a vertical direction y normal to the cooling surface, and assuming a stationary heat flow, this heat flow per surface area ϕ is

$$\phi = \lambda(T) \mathrm{d}T/\mathrm{d}y \quad \text{and} \quad \phi = (k/H_s) \ln(T_s/T_c). \tag{4}$$

Here, H_s is the local thickness of the ribbon and T_s and T_c are the absolute melting temperature of silicon and the temperature at the silicon–wheel interface.

The temperature T_c is given by

$$(T_c - T_w)/(T_s - T_c) = (\lambda_{Si} \rho_{Si} C_{Si} / \lambda_w \rho_w C_w)^{1/2} \tag{5}$$

with λ the heat conductivity and C the specific heat of the respective materials. Strictly spoken, this formula is only valid for two infinitively large pieces of material which are brought into perfect heat contact. In the case of solidification of silicon on a copper wheel, T_c is about 525 K.

The main contribution to the heat flow ϕ comes from the heat of solidification L which amounts to 1.8×10^3 J/g. So the increase of the ribbon thickness during the transport in the x-direction by the wheel is approximately

$$\mathrm{d}H_s/\mathrm{d}t = \phi/\rho_s L \quad \text{or} \quad H_s \mathrm{d}H_s/\mathrm{d}x = (k/\rho_s L v_w) \ln(T_s/T_c), \tag{6}$$

where v_w is the velocity of the wheel. The thickness H_s at the end of the puddle, at $x = x_0$, is

$$H_s = \{2kx_0 \ln(T_s/T_c)/\rho_s L v_w\}^{1/2}. \tag{7}$$

This approximation can be improved by adding one term for enthalpy decrease of the liquid silicon during cooling to the melting point and another term for cooling the ribbon material to a mean temperature of about $\frac{1}{2}(T_s + T_c)$. The contributions of these terms are much smaller than the contribution of the solidification heat. The heat flow to the surroundings by radiation and convection can be neglected. Concluding, the thickness of the solid ribbon, formed at the bottom of the puddle, is

$$H_s = \{2kx_0 \ln(T_s/T_c)/\rho_s v_w (L + C_l(T_r - T_s) + \tfrac{1}{2} C_s (T_s - T_c))\}^{1/2}. \tag{8}$$

Substitution of numerical values yields

$$H_s \approx 3.8 \times 10^{-3} (x_0/v_w)^{1/2}, \quad \text{in SI.} \tag{9}$$

Mostly, the solid ribbon leaving the puddle is covered by a thin layer of liquid silicon. To account for this phenomenon, a description of the momentum transport from the wheel to the liquid puddle is needed. Hideo Shingu et al. [5] calculated the velocity distribution in a liquid puddle on a rotating wheel by solving the equations

$$u\frac{\partial u}{\partial x} + v\frac{\partial u}{\partial y} = \nu\frac{\partial^2 u}{\partial y^2} \quad \text{and} \quad \frac{\partial u}{\partial x} + \frac{\partial v}{\partial y} = 0. \tag{10}$$

The boundary conditions are $u = v_w$ and $v = 0$ at $y = 0$ and $u = 0$ at $y = \infty$. Here u and v are the velocities in $x-$ and y-direction, respectively. The wheel surface corresponds with $y = 0$ and the front of the puddle is at $x = 0$. The solution of the equations yields a velocity distribution in an infinitely large puddle.

For our purpose, the solution can be approximated by

$$u/v_w = \exp\left\{-\left[0.7y(v_w/\nu x)^{1/2}\right]\right\}. \tag{11}$$

The thickness of the liquid silicon layer which is extracted from the puddle can be estimated by computing the thickness of the momentum boundary layer in the puddle. This boundary layer has to be defined as the layer in which u/v_w is larger than a more or less arbitrary value, e.g. $1/e$. We can also compute the thickness of the liquid layer directly, provided three assumptions are allowed. The liquid velocity at the end of the puddle has to be the same as if the puddle dimensions were more extended. No surface tension effects have to be taken into account. When all liquid silicon has been accelerated to v_w, the liquid film thickness becomes

$$H_l = \int_0^\infty u/v_w \mathrm{d}y, \tag{12}$$

at least if we also neglect the development of the solid ribbon. We deduced the value of 0.94×10^{-6} m^2/s for the kinematic viscosity ν from the value of the dynamic viscosity as adopted by Kodera [8]. With this value, eqs. (11) and (12) yield

$$H_l = 1.4 \times 10^{-3} (x_o/v_w)^{1/2}, \quad \text{in SI.} \tag{13}$$

Comparison of eqs. (9) and (13) shows that an important part of the liquid silicon which has been accelerated in the front of the puddle must be frozen in at the end of the puddle. A lower limit for the amount of extracted liquid silicon is found by eq. (12) if the integration range is not chosen from the wheel surface but from the height $y = H_s$ of the already solidified ribbon. Then the typical thickness of the liquid film at optimal stability is less than 5 μm, whereas eq. (13) yields extracted liquid layers of 30 μm and more. With these results our experiments can be explained as far as the temperature and the momentum boundary layers are concerned.

The first objective of our experiments was to determine a region of process parameters in which stable and reproducible ribbons could be produced. About 130 casting experiments were carried out, 80 of which were suitable for the determination of the stable region. We define the stability as the ratio B_m/B_c of a measured

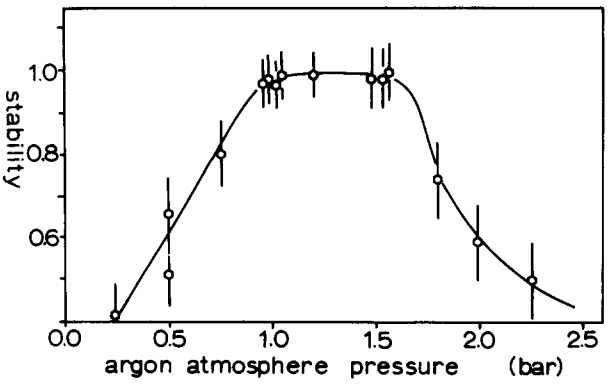

Fig. 2. Stability of jet casting as a function of the ambient gas pressure.

and a computed ribbon parameter,

$$B_m = WH\rho_s \quad \text{and} \quad B_c = \pi R^2 (2\rho_l \Delta p)^{1/2} / v_w, \tag{14}$$

with W the width and H the thickness of the ribbon. These parameters have to be equal to the mass of the ribbons per unit length. Instability usually manifests itself by scattering of liquid silicon droplets. These droplets do not contribute to the solid ribbon. Consequently the ratio B_m/B_c is equal to one or less.

The casting apparatus was placed in a vacuum chamber in which after evacuation the pressure could be selected between 0 and 2.5 bar by filling with argon. It was found that this gas helps to stabilize the silicon flow, and stable castings occurred between 1.0 and 1.5 bar (absolute) as can be seen in fig. 2. Fig. 3 shows that the angular velocity of the wheel of 30 cm in diameter had to be chosen between 600 and 1200 rpm. A wide range of mass flows were examined by applying various ejection pressures. As shown in fig. 4, the maximum mass flow for stable casting was 6 g/s.

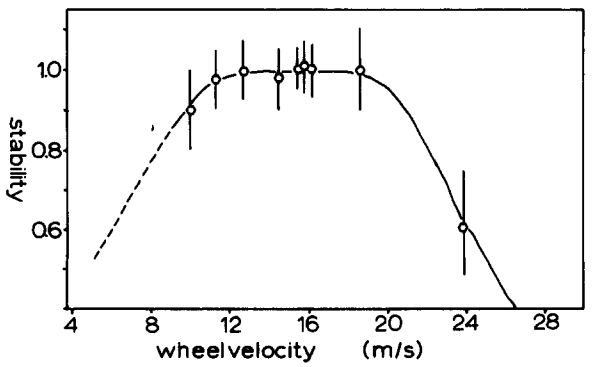

Fig. 3. Stability of jet casting as a function of the wheel velocity.

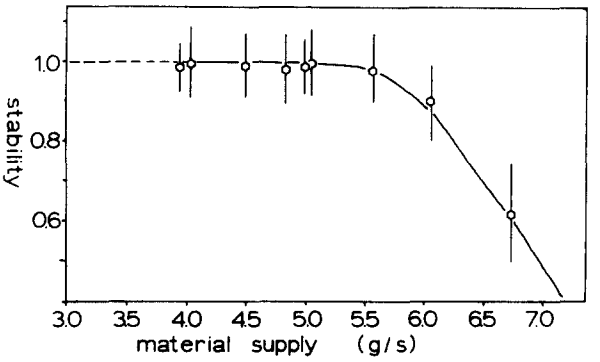

Fig. 4. Stability of jet casting as a function of the material supply.

Secondly we studied the influence of the various process parameters on the ribbon dimensions. Obviously these dimensions depend on the size of the puddle which in its turn is determined by the mass flow and the wheel velocity. Several authors studied puddle dimensions. They found that the puddle length was about inversely proportional to the square root of the wheel velocity. See for instance Katgerman et al. [9]. Others use in computations a constant puddle width to length ratio. We give here a more complicated description of the jet casting. Fig. 5 shows the ribbon thickness as a function of the mass flow and the wheel velocity for a jet of 1 mm in diameter.

The thickness of the ribbon shows a sharp minimum at about 5 g/s. This minimum thickness corresponds to a maximum width of the ribbon, since its

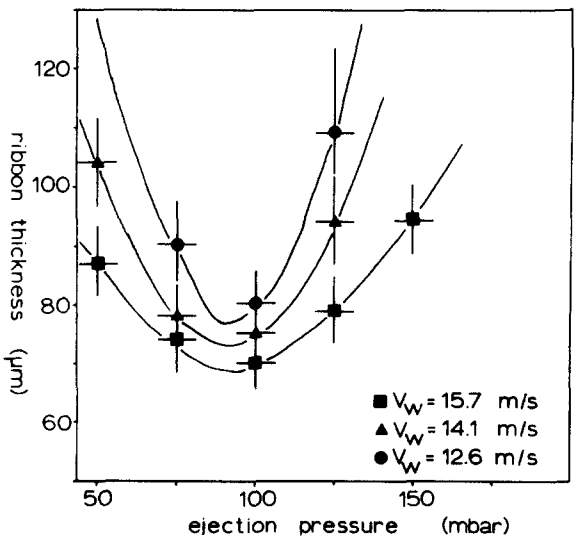

Fig. 5. Ribbon thickness as a function of the material supply at three different wheel velocities.

dimensions are related by

$$Q = WHv_w\rho_s. \tag{15}$$

At the lower flow rates, the width of the puddle strongly increases with mass flow. When the ejection pressure increases from 50 to 100 mbar the width of the ribbon increases from 1.0 to 2.4 mm. In this range a substantial puddle is developing. At the higher flow rates, the puddle is more elongated again or liquid silicon is dragged out of the puddle by the solid ribbon. An optimal stability appears to exist at a minimum ribbon thickness.

The ribbon thickness depends on the wheel velocity as shown in table 1. If we adopt the empirical relation

$$x_0 = 0.026v_w^{-1/2}, \quad \text{in SI}, \tag{16}$$

based on puddle length measurements and on theoretical considerations [9], eq. (9) yields

$$H_s = 0.60 \times 10^{-3}v_w^{-0.75}, \quad \text{in SI}. \tag{17}$$

This relation for the solid ribbon is in good agreement with the one at optimal stability. We conclude that at the extremum very little liquid silicon is dragged out of the puddle. The increase of ribbon thickness at higher flow rates cannot be accounted for by increase of the puddle length alone and we suppose that a liquid layer of about 10 to 30 μm is pulled out of the puddle at these flow rates.

It should be noted that the angle of incidence θ of the jet with respect to its projection on the wheel surface is also an important parameter. The results presented here are obtained at an angle of 65°. Other measurements at 78° and 90° are in agreement with the proportionality as found by Kavesh [3], yielding

$$H_s = 53(1 - \cos\theta)^{-1/2}\ \mu\text{m}, \tag{18}$$

at optimal stability and a wheel velocity of 15.7 m/s.

3. Flow casting

The flow casting process is different from the jet casting process in that the tip of the quartz tube is placed very close to the wheel surface so that the nozzle contacts the liquid silicon puddle. A typical case of flow casting is shown in fig. 6. The tube is

Table 1
Ribbon thickness $H_s + H_1$ as a function of the wheel velocity v_w

Δp (mbar)	Q (g/s)	$H_s + H_1$ (mm) (v_w in m/s)
75	4.8	$0.78v_w^{-0.87}$
100	5.5	$0.60v_w^{-0.79}$
125	6.2	$1.60v_w^{-1.08}$

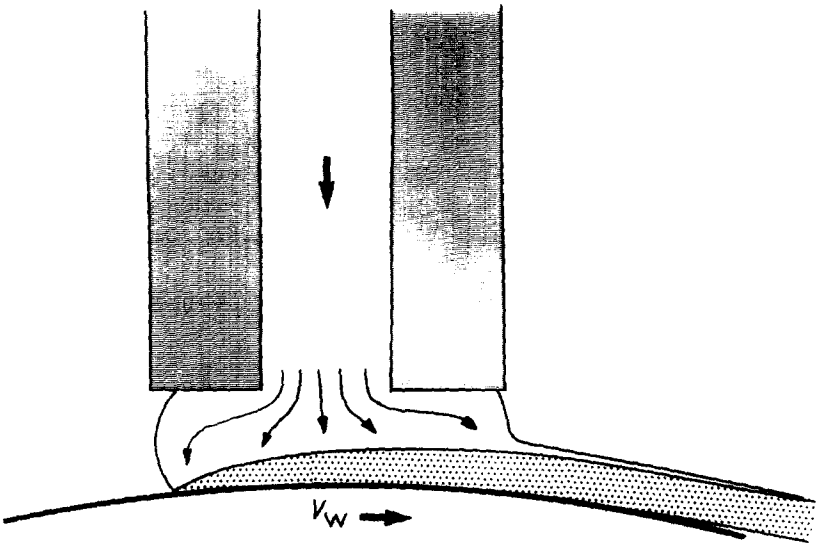

Fig. 6. Flow casting from a cylindrical shaped ejection tube.

a circular cylinder and the smallest cross section of the liquid flow normal to the flow lines is where it enters the gap between the quartz tip and the wheel surface. According to Bernoulli's law, the mass flow is now about

$$Q = 2\pi\beta R_0 H_t (2\rho_l \Delta p)^{1/2} \tag{19}$$

with H_t the distance between the quartz tip and the cooling surface. The factor β is introduced to account for the fact that part of the distance H_t is occupied by the developing solid silicon layer. Therefore β is always less than but close to unity. For a first-order estimation of β we neglect the momentum boundary layer of the liquid silicon and assume the flow to be equally divided in all directions along the cooling surface. Hence, the thickness of the solid layer underneath the tube opening must be about half the final thickness of the ribbon H leading to

$$\beta \approx \left(H_t - \tfrac{1}{2}H\right)/H_t. \tag{20}$$

The presence of the nozzle has a strong stabilizing influence on the process. Mass flows up to 20 g/s are easily realized, since the flow casting puddle can become much wider than the jet casting puddle. Measurements on our flow casting ribbons have led to the empirical relation

$$H = (2.5 \times 10^{-3})(W/v_w)^{1/2}, \quad \text{in SI.} \tag{21}$$

This is in agreement with eq. (9), if the ratio of the length x_0 and the width W of the puddle is constant for flow casting.

In preliminary experiments we made ribbons of 5 to 9 mm width and 30 to 50 μm average thickness, but we expect that production of wider and thicker ribbons is very well possible. Of course, changes in distance of the quartz tip to the wheel strongly affect the dimensions of the ribbon and a fast automatic distance control would be necessary for large production processes.

4. Grain growth

The grain size of the ribbons can be improved by annealing. The polycrystalline material exhibits considerable grain growth on annealing. This is characteristic of material which has been grown out of the liquid phase. Polycrystalline material produced by a gas phase reaction usually shows no grain growth after recrystallization.

The driving force for grain growth is the grain boundary free energy, which decreases by the reduction of the area of the grain boundaries. Generally, the velocity of a moving grain surface is expressed by the driving pressure F and the mobility m:

$$v = Fm \quad \text{with} \quad F = \gamma_b/a, \tag{22}$$

where γ_b is the surface free energy. The quantity $1/a$ is either the curvature of a grain boundary or, by approximation, the ratio of the grain boundary area and the volume of the grains. In the latter case, a is proportional to the diameter of the grains. The proportional factor depends on the shape of the grains which may be approximated by e.g. cubes, cylinders or balls. Since the shape of the grains of quenched ribbons are rather long with respect to their diameter, we will describe these grains as having a cylindrical shape. With the definitions mentioned above, one can now deduce for the diameter of a growing grain as a function of time $d(t)$:

$$d^2(t) - d^2(0) = 8m\gamma_b t. \tag{23}$$

The thermal activation of the mobility with activation energy E is expressed by

$$m = m_0 \exp(E/kT). \tag{24}$$

Grain-growth experiments have been performed at three temperatures with anneal-

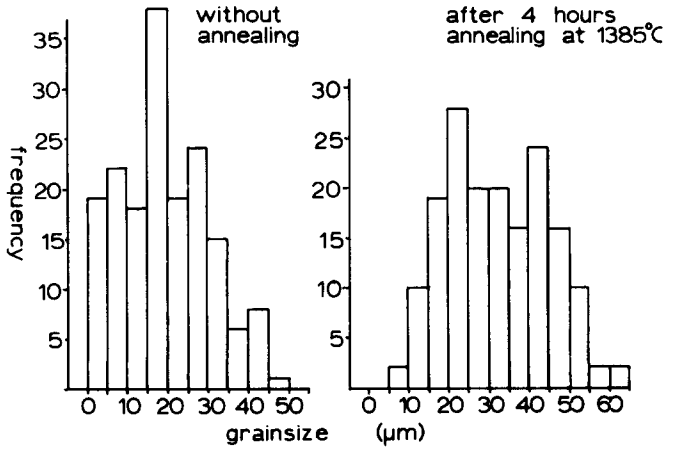

Fig. 7. Histograms of the grain diameter distribution at the surface of a ribbon before and after grain growth during annealing.

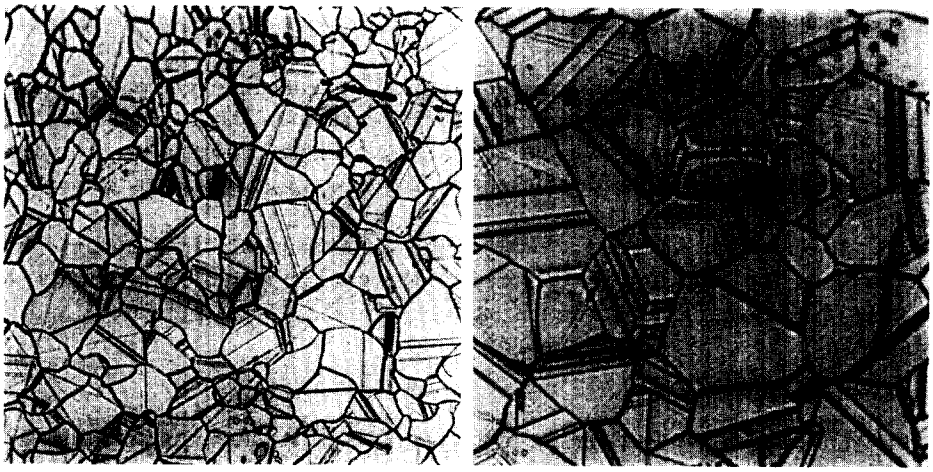

Fig. 8. Grain shapes at the surface of a ribbon before and after anneling during 4 h at 1385 °C. The photographs show a part of about 0.3×0.3 mm^2 of the ribbon surface.

ing times between 4 and 38 h. The square of the mean diameter has been determined as a function of time. Fig. 7 shows the grain-size distributions before and after annealing at 1385 °C. In fig. 8 the shapes of the grains are shown. If γ_b is estimated to be 2 J/m^2, the mobilities are as given in fig. 9. The activation energy of the mobility is (4.4 ± 0.7) eV. In fig. 9 the results are also compared with those of Schins [11] on recrystallization of CVD grown silicon and on grainboundary migration in bicrystals.

The experiments confirm that grain growth can be achieved at relatively high temperatures.

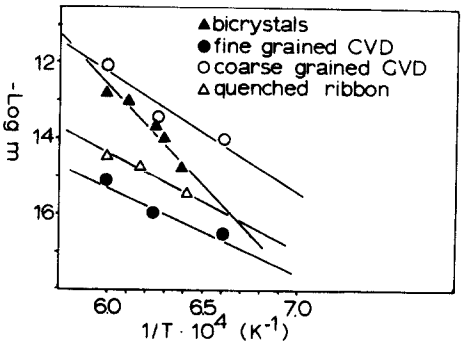

Fig. 9. Decimal logarithm of the mobility m in m^3/Ns of grain boundaries in quenched ribbons, compared to results of Schins on recrystallization of CVD grown polycrystalline silicon and on the grain boundary mobility in bicrystals [11].

5. Prospects for application of the casting technique

The quality of the ribbon material, the ribbon dimensions and the growth rate are of paramount importance to assess the suitability of the jet casting or flow casting technique for large scale production. The ribbons which we have grown have a sufficient thickness for solar cells. Somewhat thicker ribbons might be stronger, but they cannot be bent like the thinner ones. The ribbons in our experiments are less than 1 cm wide but the widths can be increased to several cm, as is confirmed by Arai et al. [1]. In the case of flow casting one can realize wider ribbons by using an ejection tube with a slit opening or an array of small holes. Even in the case of jet casting a set of parallel jets can be applied to increase the ribbon width. Fig. 10 shows two pieces of a ribbon, one produced by flow casting and one produced by three parallel jets whose puddles just overlapped. In this way the latter ribbon was made about 2.5 times as wide as a ribbon from a single jet. Only small fragments of the triple jet ribbons were produced. These ribbons sticked somewhat longer to the wheel than single jet ribbons and consequently they missed the ribbon catching tube and cracked against the wheel vessel. When a sufficiently large catching tube is positioned properly, there is probably no principal limitation to the length of the ribbons. More development work could be done to wind these ribbons or to cut them continuously during production. Such methods are known in metallurgy and thread manufacturing industries. The production velocity of the fast casting methods is incomparable to any other ribbon growth technique. However, the grain size is very small.

The final, and we think the decisive criterion for application is the quality of the ribbons. This quality is determined by the purity of the material, the size of the grains and the properties of the grain boundaries. The purity of the starting material

Fig. 10. Quenched ribbons on a 2.5 mm grid. The ribbon at the top was produced by triple jet casting and the wider ribbon at the bottom was made by flow casting. The average thickness of the upper ribbon was 0.110 mm and that of the lower 0.042 mm.

Fig. 11. Cross section of a ribbon produced by jet casting. The ribbon is about 0.08 mm thick.

could be lost by contamination during the casting process. Using a metal (copper) wheel, the contact temperature is rather low so little contamination is expected. Analysis by RBS with a resolution of better than 100 ppm did not show copper impurities near the surface. Also undoped silicon maintained its high resistivity after a casting process.

The grains in the ribbons have a columnar shape, as shown in fig. 11. This shape is advantageous for a photovoltaic device. To obtain a 10% efficiency, the grain diameter must be at least about 0.1 mm, as shown for instance by Ghosh et al. [10]. Efficiency is lost by traps and recombination centers at the grain boundaries. Of course other negative influences like short circuiting due to the presence of grain boundaries may further decrease the efficiency. As we have shown, grain growth in cast silicon is significant. This grain growth is fundamentally different from recrystallization of CVD grown material, as shown by Jain et al. [12] and Schins et al. [13]. In CVD material no grain growth is observed after recrystallization. The shape of the final grains is quite different from the polygon-like shape of the grains in cast silicon. Although more research is necessary, the results so far seem worthwhile for further investigation on ribbon production by fast casting and recrystallization.

6. Conclusions

The jet casting and flow casting of silicon are well understood in terms of thermal transport and momentum transport in a liquid puddle. If developing independently, the solid ribbon pulled out of the puddle would be about three times as thick as the liquid layer. Both solid and liquid layers would grow in thickness proportional to the square root of the length of the puddle. Consequently the momentum boundary is almost totally frozen in short puddles. A thicker momentum boundary layer develops on top of the solid ribbon in longer puddles. Stability of the casting methods has been studied as a function of wheel velocity, ambient gas pressure and mass supply. Within certain limits solid ribbons develop underneath a stable puddle. Grain size can be improved by grain growth close to the melting temperature. The activation energy was found to be (4.4 ± 0.7) eV, the mobility amounted to 3×10^{-15} m^3/Ns at 1385 °C. Due to the fast ribbon growth and the possibility of grain growth, jet casting and flow casting are expected to be promising methods for production of polycrystalline silicon solar cells. However, more experiments are needed to study grain growth as well as grain boundary behaviour in solar cells. Also more development work is necessary to produce wider and longer ribbons.

References

[1] K.I. Arai, N. Tsuya and T. Takeuchi, 14th IEEE Photovoltaic Specialists Conf., San Diego (1980) p. 31.
[2] R.V. Raman and A.F. Witt, in: Rapidly Solidified Amorphous and Crystalline Alloys, eds. B.H. Kear, B.C. Giessen and M. Cohen (Elsevier, Amsterdam, 1982) p. 141.
[3] S. Kavesh, Metallic Glasses, Am. Soc. for Metals (1978) p. 36.
[4] T.R. Anthony and H.E. Cline, J. Appl. Phys. 49 (1978) 829.
[5] P. Hideo Shingu, K. Kobayashi, R. Suzuki and K. Takeshita, Proc. 4th Intern. Conf. on Rapidly Quenched Metals, vol. I, Sendai (1981) p. 57.
[6] D. Pavuna, J. Non-Crystalline Solids 37 (1980) 133.
[7] H.H. Liebermann, J. Mater. Sci. 15 (1981) 2771.
[8] Hiroshi Kodera, Japan. J. Appl. Phys. 2 (1963) 212.
[9] L. Katgerman and P.J. van den Brink, Proc. 4th Intern. Conf. on Rapidly Quenched Metals, vol. I, Sendai (1981) p. 61.
[10] A.K. Ghosh, C. Fishman and T. Feng, J. Appl. Phys. 51 (1980) 446.
[11] W.J.H. Schins, Thesis Utrecht (1982).
[12] G.C. Jain, B.K. Das and S.P. Bhattacherjee, Appl. Phys. Lett. 33 (1978) 445.
[13] W.J.H. Schins, J. Bezemer, H. Holtrop and S. Radelaar, J. Electrochem. Soc. 127 (1980) 1193.